Kobe University Repository : Kernel

PDF issue: 2025-12-05

Symmetry and entropy of biological patterns: Discrete Walsh functions for 2D image analysis

Yamasaki, Kazuhito

Nanjo, Kazuyoshi Z.

Chiba, Satoshi

(Citation)
BioSystems,103(1):105-112

(Issue Date)
2011-01

(Resource Type)
journal article

(Version)
Accepted Manuscript

(Rights)
© 2010 Elsevier Ireland Ltd.
This manuscript version is made available under the CC-BY-NC-ND 4.0 license
http://creativecommons.org/licenses/by-nc-nd/4.0/

(URL)
https://hdl.handle.net/20.500.14094/90006373

*Manuscript
Click here to view linked References

Symmetry and entropy of biological patterns: discrete Walsh functions for 2D image analysis

Kazuhito Yamasaki[a,*], Kazuyoshi Z. Nanjo[b], Satoshi Chiba[c]

[a] *Department of Earth and Planetary Sciences, Faculty of Science, Kobe University, Nada, Kobe 657-8501, Japan*
[b] *Earthquake Research Institute, University of Tokyo, 1-1-1, Yayoi, Bunkyo-ku 113-0032 Tokyo, Japan*
[c] *Department of Ecology and Evolutionary Biology, Graduate School of Life Sciences, Tohoku University, Aobayama, Sendai 980-8578, Japan*

Abstract

To quantify symmetry and entropy inherent in the discrete patterns such as spatial self-organization in cell sorting and mussel bed ecosystems, we introduce the discrete Walsh analysis. This analysis enables us to estimate the degree of the complicated symmetry, and to extract the symmetry from the pattern that seems to be the asymmetric. The results obtained in this paper are summarized as follows. (I) The geometrical patterns of the cell sorting become systematic with the predominance of the particular symmetry. This implies that not only the entropy but also the particular symmetry can decrease in the biological process. (II) The magnitude of the symmetry is related to the absolute value of the adhesion, and the type of the symmetry is related to the sign of the adhesion. That is, centro-symmetry dominates in the cell sorting pattern caused by large negative adhesion, and double symmetry dominates in the pattern caused by large positive adhesion. (III) Spatial self-organization in mussel bed is accompanied by the decreasing of the centro-symmetry. This implies that the positive "adhesion" between mussel individuals increases with time. (IV) In the biological process, the Curie symmetry breaking occurs at intervals.

Keywords: Walsh analysis, symmetry, entropy, symmetropy, image analysis, Curie symmetry breaking

*Corresponding author. Fax: +81-78-803-5757
Email address: yk2000@kobe-u.ac.jp (Kazuhito Yamasaki)

1. Introduction

Biological patterns often show discrete patterns consisting of a regular grid of cells such as animal stripe pattern and shell pigment patterns (e.g., Wolfram, 2002). Each of the cells can be in one of several "states". In this paper, we take up a two-state model, in which each of the cells can be "On" and "Off" (or "Black" and "White"). Moreover, biological patterns also show discrete structure that induces a symmetry breaking (e.g., Turing, 1952). Therefore, the concept of the symmetry is a useful tool to quantify and classify the discrete biological patterns. Especially, bilateral symmetry, spherical symmetry and radial symmetry are often recognized in the patterns. This paper quantifies the more complicated symmetry that can not be easily recognized, and extracts the symmetry that hides behind the asymmetric pattern. For this analysis, we suggest a mathematical tool: the discrete Walsh analysis.

Now, in biology that deals with waveforms and signals, the Fourier analysis has been known as a tool for decomposing a function into simpler trigonometric functions (Fig. 1A). As we will see in the Section 2.2, the discrete Walsh analysis decompose the two-dimensional discrete pattern into simpler trigonometric patterns called discrete Walsh functions (Fig. 1B). Based on the Walsh functions, we can easily estimate the degree of the symmetry inherent in the discrete patterns (e.g., Yodogawa, 1982; Nishiyama et al., 2008; Yamasaki and Nanjo, 2009).

Moreover, to quantify the randomness of a pattern, we introduce information entropy. Although the concept of entropy plays an important role in biological process, it has been ignored in the previous Walsh analysis applied to physical process (e.g., Nishiyama et al., 2008; Yamasaki and Nanjo, 2009). In physical system such as a solid-state phase transition, the decrease in thermodynamic entropy directly corresponds to the symmetry breaking as the temperature is lowered (Rutherford, 2001; Avalos, et al., 2004). Then, we consider how the symmetry is related to the entropy in the biological phase transition.

As an example of the discrete pattern, we take up spontaneous cell sorting caused by cell-cell adhesion. Mochizuki et al., (1996) analyzed cell sorting caused by the cell-cell adhesion in limb-formation based on computer simulations of spatial Markov processes on a 2-D lattice (Fig. 2). According

to their model, the transition from homogeneous cell pattern (Fig. 2C) to inhomogeneous one (Fig. 2E∼H) is abrupt. The condition for this abrupt transition can be computed by translating the standard results in equilibrium statistical thermodynamics into the context of cell sorting. In this case, the spontaneous cell sorting can be regarded as one of the phase transition of the two-dimensional discrete patterns.

Moreover, we take up the experimental data for spatial self-organization in mussel bed ecosystems (Koppel et al., 2008). Spatial self-organization is the main theoretical explanation for the global occurrence of regular or otherwise coherent spatial patterns in ecosystems. Under homogeneous laboratory conditions, mussels developed regular patterns, similar to those in the field (Fig. 3). An individual-based model derived from the experiment showed that interactions between individuals explained the observed patterns.

The structure of this paper is as follows. In Section 2, we explain data on cell sorting patterns and method: Walsh analysis for calculating entropy and symmetry of the patters. Since Fourier analysis is more familiar than Walsh analysis in biology, we express the Walsh analysis in terms of the Fourier (sine-cosine) functions. In Section 3, we describe results. In Section 4, we discuss results and consider the relationship between entropy and symmetry of the 2D discrete patterns.

2. Data and methods

2.1. Data

The entropy and the symmetry of discrete patterns can be estimated by using the discrete Walsh analysis (Yodogawa, 1982). In this paper, we use the results of the computer simulation for the cell sorting (Mochizuki et al., 1996), and the experimental data for spatial self-organization in mussel bed ecosystems (Koppel et al., 200), because they are suitable for applying the discrete Walsh analysis used in the previous papers (Nanjo et al., 2006; Nishiyama et al., 2008; Yamasaki and Nanjo, 2009). Details are as given below.

2.1.1. Cell sorting

To relate the observed degree of sorting and the strength of cell-cell adhesion, Mochizuki et al., (1996) studied a stochastic spatial model of cell sorting, which is mathematically equivalent to a quenched binary alloy in

physics. They consider cells arranged on a two-dimensional regular square lattice, in which there are two kinds of cells, called black and white cells.

The model can be characterized by two parameters: differential adhesion A and cell motility m. Cells move randomly by exchanging their locations between nearest neighbors in a time interval of length $\triangle t$ with probability $m\triangle t$. The adhesion of cells is assumed to occur only between cells in contact. Let λ_{BW}, λ_{BB}, and λ_{WW} be the strength of adhesion per cell contact between a black and a white cells, between two black cells, and between two white cells, respectively. In this case, differential adhesion is defined as $A = \lambda_{BB} - 2\lambda_{BW} + \lambda_{WW}$, which determines the tendency of sorting-out of the cell population (see Mochizuki et al., 1996 for more details.). Some examples of the simulation results are given in Fig. 2, which will be used in this paper.

The cell sorting patterns depend on the ratio A/m. If A/m is sufficiently large, the pattern is inhomogeneous, i.e., coarse grained cell sorting occur, in which the whole system is separated into subareas (see Fig. 2E$\sim$2H). On the other hand, for small A/m, the pattern is homogeneous, i.e., subareas include similar densities of black cells (see Fig. 2C and 2D). Transition from homogeneous pattern to inhomogeneous one is abrupt and the condition is given by unstable uniform solution (Mochizuki et al., 1996): $\rho_B(1-\rho_B) > m/(4A)$, where ρ_B is fraction of black cells. In this paper, we use the data illustrated by Fig. 2, in which $\rho_B = 0.5$, so this unstable solution becomes

$$\frac{A}{m} > 1. \tag{1}$$

Eq. (1) shows that the transition occurs when differential adhesion A is larger than cell motility m in the case of $\rho_B = 0.5$.

2.1.2. Mussel bed ecosystems

Koppel et al., (2008) studied the pattern formation by using mussels in the laboratory within a $130 \times 90 \times 27$ cm polyester container filled with seawater. Mussels were obtained from wooden wave-breaker poles on the beaches near Vlissingen, the Netherlands (51.458713N, 3.531643E). In the experiments, mussels were laid-out on an 80×60 cm surface of either concrete tiles. Mussels were evenly distributed at the start of the experiments, after which mussel movement was determined from the images by tracking the position of the mussels. In this paper, we take up the time-laps movie (1163952S2) showing the formation of spatial patterns by approximately 1200 mussels. In this paper, the central patterns of mussel bed were covered with $2^5 \times 2^5$ cells. If

we find a part of or whole of mussel bed in a cell of (i, j), then the cell is recognized as the black cell ($x_{ij} = 1$), otherwise the white cell ($x_{ij} = 0$).

2.2. Method

The order of the discrete Walsh analysis is as follows. (i)Spatial pattern is considered as an information source consisting of dot patterns. The dot patterns emitted from the source are assumed to occur with the corresponding probabilities given by Eq. (3). Entropy function in information theory is applied to the probabilities so that we can define entropy by Eq. (6) or Eq. (13). (ii)When spatial pattern is regarded as an information source consisting of four types of symmetry (Fig. 4B), the corresponding probabilities are given by Eqs. (8) to (11). In this case, we can define the entropy concerned with symmetry by Eq. (12). This is called symmetropy. (Strictly speaking, this symmetropy corresponds to "partial symmetropy" (Yamasaki and Nanjo, 2009). For simplicity, we use the term "symmetropy" in this paper.)

As details of the mathematical procedures were given in previous papers (e.g., Yodogawa, 1982; Nishiyama et al., 2008), only a brief outline is described below. Following Yodogawa (1982), we represent Walsh function based on sinusoidal functions (see also Beauchamp, 1975). Walsh function $\mathrm{wal}(\kappa, \chi)$ of order κ and argument χ can be represented in terms of the Fourier (sine-cosine) functions: $\mathrm{wal}(\kappa, \chi) = \prod_{i=0}^{m-1} \mathrm{sgn}[(\cos 2^i \pi\chi)^{\kappa_i}]$, where $0 \leq \chi < 1$, $\kappa = 0, 1, \cdots$ and $\kappa_i = 0$ or 1. The function $\mathrm{sgn}[t]$ is -1 if $t < 0$ and $+1$ if $t \geq 0$. The product of the two walsh functions is given by dyadic addition of orders (nonnegative integers): $\mathrm{wal}(\lambda, \chi)\mathrm{wal}(\kappa, \chi) = \mathrm{wal}(\lambda \oplus \kappa, \chi)$. Since the Walsh functions form a complete orthonormal set in the interval $0 \leq \chi < 1$, every integrable functions $f(x)$ can be expressed as a series of the form $f(x) = \sum_{i=0}^{\infty} a_i \mathrm{wal}(i, \chi)$, where the coefficients a_i are given by $a_i = \int_0^1 f(x)\mathrm{wal}(i, \chi)d\chi$.

Discrete Walsh functions are defined below. Let the interval $(0, 1)$ be divided into $N = 2^q$ (q is a positive integer) with equal subintervals. Let $w_n(i)$ be the value of the nth order Walsh function in the ith subinterval. In this case, the two-dimensional discrete Walsh function is defied as $W_{mn}(i, j) = w_n(i)w_m(j)$ on a square region divided into equal square subregions called cells (Fig. 4A; see also p. 573 in Wolfram, 2002). These functions can be represented in matrix form as $[W_{mn}(i, j)]$, where $W_{mn}(i, j)$ is the value of the (m, n)th order Walsh function in the ith row cell in the jth column.

Patterns used in this paper are restricted to square matrices, each consisting of $N \times N = 2^5 \times 2^5$ square cells. This pattern can be written as $[x_{ij}]$,

where x_{ij} is the value of gray level in the ith row cell in the jth column and $i, j = 0, 1, \cdots, N-1$. If there are just two gray levels: for instance "black" and "white", x_{ij} is usually represented by 1 and 0, respectively. The two-dimensional discrete walsh transform of the pattern $[x_{ij}]$ is given by

$$a_{mn} = \frac{1}{N^2} \sum_{i=0}^{N-1} \sum_{j=0}^{N-1} x_{ij} W_{mn}(i, j), \tag{2}$$

where $m, n = 0, 1, 2, \cdots, N-1$. The functions a_{mn} and $(a_{mn})^2$ are the two-dimensional Walsh spectrum and power spectrum, respectively. Since $a_{00} = (1/N^2) \sum_{i=0}^{N-1} \sum_{j=0}^{N-1} x_{ij}$, we can interpret a_{00} as the average value for the summation of gray levels in the pattern $x[i, j]$.

The Walsh power spectrum can be normalized:

$$p_{mn} = \frac{(a_{mn})^2}{K}, \tag{3}$$

with

$$K = \sum_{m=0}^{N-1} \sum_{n=0}^{N-1} (a_{mn})^2 - (a_{00})^2. \tag{4}$$

The reason for subtracting a_{00} from the summation is that W_{00} provides no shape information (see Fig. 4A, $m = n = 0$). In this case, we obtain

$$\sum p_{mn} = 1, \tag{5}$$

where the sum is taken over all ordered pairs (m, n) except $(0, 0)$ for $0 \leq m, n \leq N-1$.

Applying the entropy function in information theory to the normalized power spectrum p_{mn}, we obtain information entropy concerned with the pattern:

$$E = -\sum_{m=0}^{N-1} \sum_{n=0}^{N-1} p_{mn} \log_2 p_{mn}. \tag{6}$$

If the value of a certain component is larger than the values of the other components, Eq. (6) shows that E decreases, i.e., the pattern becomes systematic. On the other hand, if the values of the components are almost equal each other, E increases, i.e., the pattern becomes random.

Next, let us consider the information entropy concerned with symmetry of the pattern. Because the two-dimensional Walsh functions can be easily divided into four types of symmetry (Fig. 4B), Eq. (5) can be rewritten as

$$\sum_{i=1}^{4} P_i = 1, \tag{7}$$

where

$$\text{vertical symmetric component: } P_1 = \sum_{\substack{m=\text{even},\\ n=\text{odd}}} p_{mn}, \tag{8}$$

$$\text{horizontally symmetric component: } P_2 = \sum_{\substack{m=\text{odd},\\ n=\text{even}}} p_{mn}, \tag{9}$$

$$\text{centro-symmetric component: } P_3 = \sum_{\substack{m=\text{odd},\\ n=\text{odd}}} p_{mn}, \tag{10}$$

$$\text{double symmetric component: } P_4 = \sum_{\substack{m=\text{even},\\ n=\text{even}}} p_{mn}. \tag{11}$$

Applying the entropy function in information theory to these four symmetric components, we obtain

$$S = -\sum_{i=1}^{4} P_i \log_2 P_i. \tag{12}$$

Since this entropy is concerned with symmetry, it is called symmetropy (Yodogawa, 1982). The symmetropy means the entropy of information source consisting of the four types of symmetry, and can be considered as a quantitative and objective measure of symmetry. If the value of a certain component is larger than the values of the other three components, the pattern is rich in symmetry related to the certain component. In this case, Eq. (12) shows that S decreases. On the other hand, if the values of the four components are almost equal each other, the pattern is poor in symmetry and S increases.

Eqs. (7) and (12) show that S ranges form 0 to 2 bits. On the other hand, Eq. (6) shows that the minimum value of E is zero bits, but the maximum value depends on the number of the cell: $\log_2(N^2 - 1)$. (Since we ignore the component a_{00}, the total number of cell is $N^2 - 1$.) Then, let us define the normalized entropy E_n as follows:

$$E_n = \frac{E}{\log_2(N^2 - 1)}. \tag{13}$$

In this case, E_n ranges from 0 to 1 bit.

2.3. Examples

For example, take two patterns shown in Fig. 5B and C. In Fig. 5B, the two dimensional Walsh spectra calculated by Eq. (2) are given by $a_{00} = 0.5, a_{10} = a_{13} = a_{22} = -0.25, a_{21} = 0.25$, and all the others are zero. In this case, Eq. (4) shows $K = 0.25$. Therefore, from Eq. (3) and Eqs. (8) to (11), we obtain $p_{10} = p_{13} = p_{21} = p_{22} = 0.25$ and $P_1 = P_2 = P_3 = P_4 = 0.25$, which satisfy Eq. (5) and Eq. (7), respectively. Hence, by using Eqs. (6), (13) and (12), the entropy and the symmetropy of the pattern in Fig. 5B can be estimated as

$$E_n = 0.51, \tag{14}$$

$$S = 2.00. \tag{15}$$

On the other hand, the spectra of Fig. 5C are given by $a_{00} = 0.5$, $a_{01} = a_{21} = a_{31} = 0.25$, $a_{11} = -0.25$ and all the others are zero. In the same way as described above, the entropy and the symmetropy of Fig. 5C can be estimated as

$$E_n = 0.51, \tag{16}$$

$$S = 1.00. \tag{17}$$

It is found from Eqs. (14) and (16) that the degree of randomness of the patterns shown in Fig. 5B and C are equal each other. On the other hand, Eqs. (15) and (17) show that the symmetropy of Fig. 5B is larger than that of Fig. 5C. This means that the pattern in Fig. 5B lacks symmetry compared with the pattern in Fig. 5C. The examples described above show that symmetry of a pattern is not necessarily correlated with entropy of the pattern. However, previous studies have concentrated on the symmetry (e.g., Nishiyama et al., 2008; Yamasaki and Nanjo, 2009). In this case, we cannot quantify the difference between the patterns that have the same symmetry but the different entropy. For instance, the pattern in Fig. 5B cannot be

distinguished from that in Fig. 5D in the sense of the symmetry, although the cell in Fig. 5B is more connected with the other cells compared with that in Fig. 5D. Then, in this paper, we estimate not only the symmetry but also the entropy of the cell sorting patterns.

3. Results

Fig. 6 shows the normalized power spectrum p_{mn} of Fig. 2. It is found that the particular components of p_{mn} increase depending on the sign of A/m. That is, in the case of $A/m < 0$ (Fig. 6A and B), the values of p_{mn} with high numbers of m and n predominate, which reflects the decrease of the cluster size. In the case of $A/m > 0$ (Fig. 6D∼H), the values of p_{mn} with low numbers of m and n predominate, which reflects the increase of the cluster size.

Fig. 7A shows the entropy E_n of Fig. 2 estimated from p_{mn} in Fig. 6. The data $E_n = 0.15$ at $A/m = -2$ is not plotted in the figure, because it is too small. When A/m is smaller than the threshold value 1 (see Eq. (1)), the entropy E_n is close to the maximum value 1.0 bit which means the pattern is random. On the other hand, when A/m increases and passes the threshold value, the entropy decreases, i.e., the pattern formation occurs. Moreover, when A/m remarkably increases and passes the value 4, the entropy begins to increase, i.e., the pattern becomes random again.

The symmetry and the symmetropy of Fig. 2 are estimated, and plotted against A/m (Fig. 7). The data at $A/m = -2$: $P_1 = 0.03$, $P_2 = 0.02$, $P_3 = 0.92$, $P_4 = 0.03$ and $S = 0.54$ are not plotted in the figures, because they are quite different from the other data. When A/m passes the threshold value 1, P_3 decreases and P_4 increases as Fig. 7C shows. On the other hand, Fig. 7B shows that P_1 and P_2 do not change appreciably. Moreover, when A/m passes the value 4, P_3 remains low and P_4 begins to decrease. From these symmetric components change, the symmetropy decreases at $A/m \approx 1$ and begin to increase at $A/m = 4$ as Fig. 7A shows.

In a similar fashion described above, we estimate the entropy, the symmetry and the symmetropy of the pattern formation by mussels based on the experimental data (Koppel, et al., 2008). In Fig. 8, theses data are plotted against time. Fig. 8 shows that the entropy tends to decrease, but the symmetropy varies randomly. Figs. 8B and C show that P_3 tends to decrease, but the other symmetries are irregular.

4. Discussion

Let us discuss the relationship between the entropy and the symmetry in the biological phase transition: the cell sorting. In physical system such as a solid-state phase transition, the decrease in thermodynamic entropy directly corresponds to the symmetry breaking as the temperature is lowered (Rutherford, 2001; Avalos et al., 2004). As describe in the Section 2.3, the information entropy change is not necessarily correlated with the symmetry change. If the entropy and the symmetry correlate to each other, there are various possible combinations as follows (off course, other combinations can be created):

(i)The entropy change is correlated with the symmetry change. For example, this is a case where the pattern becomes systematic with the predominance of the particular symmetry (e.g., Fig. 5B $\rightarrow$ A).

(ii)The entropy varies and the symmetry maintains a uniform value. For example, this is a case where the pattern becomes random to maintain the degree of symmetry (e.g., Fig. 5B $\rightarrow$ D).

(iii)The symmetry varies and the entropy maintains a uniform value. For example, this is a case where the pattern restores symmetry to maintain the randomness (e.g., Fig. 5B $\rightarrow$ C).

To what combinations does the cell sorting pattern belong? Fig. 7A shows that the entropy and the symmetropy have a similar tendency to change. This result implies that the cell sorting pattern taken up in this paper belongs to the combination (i), i.e., the formation of the cell sorting is accompanied by the predominance of the particular symmetry (i.e., the decrease of the other symmetries). This means that not only the entropy but also the particular symmetry can decrease in the biological process. Details are given below.

As shown in Fig. 7A, the symmetropy decreases with the absolute value of A/m. From Eq. (12), a decrease of the symmetropy is caused by an increase of the particular symmetry. If the cell motility m is constant (Mochizuki et al., 1998), this means that the magnitude of the particular symmetry increases with the absolute value of the differential adhesion A. On the other hand, the sign of A is related to the type of the symmetry as follows. In the case of $A < 0$, the cluster size decreases and the mixed cell shows the checker-board like pattern (Figs. 2A and B). That is, the centro-symmetric component P_3 increases (Fig. 7C). This agrees with the previous results (e.g., Honda and Eguchi, 1980). Moreover, Figs. 7B and 7C show that not only P_3 but also the other symmetries: P_1 and P_4 hide behind the pattern with

the negative A. This cannot be easily recognized without the discrete Walsh analysis. In the case of $A > 0$, the cluster size increases and the mixed cell shows the segregated pattern (Fig. 2D∼H). This pattern is accompanied by the predominance of the doubly symmetric component P_4 and the decreasing of P_3 (Fig. 7C). To our knowledge, this has not been reported in detail.

Fig. 7A also illustrates that the entropy and the symmetry of the cell sorting patterns shows a fall at $A/m \approx 1$, i.e., $A \approx m$, followed by s rise at $A/m \approx 4$, i.e., $A \approx 4m$. The former threshold value has been predicted by the previous theoretical study (Mochizuki et al., 1996) such as Eq. (1), but the latter value has not. We may intuit that the more adhesion A increases, the more systematic the cell sorting patten becomes. However, contrary to this intuition, the results show the middle range $m < A < 4m$ in which the cell sorting pattern becomes extremely systematic.

Fig. 8A shows that the entropy of the distribution pattern of the mussel tends to decrease. This result provides the quantitative support for the spatial self-organization of the mussel. On the other hand, the symmetropy seems to vary randomly. From Eq. (12), this is due to the irregular patterns of the symmetries except for P_3 (Figs. 8B and C). By comparison with Fig. 7C, the decreasing of $P3$ implies that the positive "adhesion" between mussel individuals increases with time.

Finally, let us reconsider the symmetry change in the biological process from the viewpoint of the Curie symmetry principle (Curie, 1894; Rosen and Copie, 1982). In physical process, the Curie symmetry principle has been known as an aspect of the causality relationship between the symmetry of the cause and that of the resultant effect, and allows us to predict possible properties and to forbid impossible ones (e.g., Jaeger, 1920). The Curie symmetry principle is expressed in terms of the symmetropy as follows (Nanjo et al., 2005): symmetropy evaluating the cause S_{cause} is equal to or smaller than symmetropy evaluating the resultant effect S_{effect}:

$$S_{\text{cause}} \lesssim S_{\text{effect}} \tag{18}$$

Since the simulation is executed from a random initial pattern (Mochizuki et al., 1996), S_{cause} is considered to be the symmetropy of the random pattern: 2.0 bits. Since the maximum value of the symmetropy is 2.0 bits, Eq. (18) means that S_{effect} is constant at close to 2.0 bits if the Curie symmetropy principle holds. In this sense, Fig. 7A shows that the Curie symmetry principle breaks at the interval $1 < A/m < 4$, because the symmetropy decreases

from 2.0 bits. These quantitative results imply that the spontaneous cell sorting is accompanied by the spontaneous Curie symmetry breaking. Moreover, Fig. 8 shows that the Curie symmetry breaking occurs at the intervals. This finding may provides quantitative support for the idea: symmetry breaking in self-organizing systems from a viewpoint of the Walsh analysis.

5. Conclusions

The following conclusions were derived from the results and discussion. (I)In the cell sorting, the pattern's entropy and symmetry correlate to each other, i.e., the formation of the cell sorting is accompanied by the predominance of the particular symmetry. (II)The magnitude and the sign of the differential adhesion is related to the magnitude and the type of the pattern's symmetry, respectively. That is, in the case of $A < 0$, the centro-symmetry increases; in the case of $A > 0$, the double symmetry dominates. (III) Spatial self-organization in mussel bed is accompanied by the decreasing of the centro-symmetry. This implies that the positive "adhesion" between mussel individuals increases with time. (IV) In the biological process, the Curie symmetry breaking occurs at intervals.

References

Avalos, M., Babiano, R., Cintas, P., Jimenez, J.L., Palacios, J.C., 2004. Symmetry breaking: an epistemological note. Tetrahedron: Asymmetry 15, 3171-3175.

Beauchamp, K.G., 1975. Walsh Functions and Their Applications. Academic Press, London.

Curie, P.,1894. Sur la symetrie dans les phenomenes physiques, symetrie d'un champ electrique et d'un champ magnetique. J. Phys. (Paris). 3, 393-415.

Honda, H., Eguchi, G., 1980, How much does the cell boundary contract in a monolayered cell sheet? J. Theor. Biol. 84, 573-588.

Jaeger, F.M., 1920. Lectures on the Principle of Symmetry and its Applications in All Natural Sciences. Elsevier, Amsterdam.

Van de Koppel, J., Gascoigne, J.C., Theraulaz, G., Rietkerk, M., Mooij, W.M., Herman, P.M.J., 2008, Experimental evidence for spatial self-organization and its emergent effects in mussel bed ecosystems. Science 322, 739-742.

Mochizuki, A., Iwasa, Y., Takeda, Y., 1996. A stochastic model for cell sorting and measuring cell-cell adhesion. J. Theor. Biol. 179, 129-146.

Mochizuki, A., Wada, N., Ide, H., Iwasa, Y., 1998. Cell-cell adhesion in limb-formation, estimated from photographs of cell sorting experiments based on a spatial stochastic model. Dev. Biol. 211, 204-214.

Nanjo, K.Z., Nagahama, H., Yodogawa, E., 2005. Symmetropy of fault patterns: quantitative measurement of anisotropy and entropic heterogeneity. Math. Geol. 37, 277-293.

Nanjo, K.Z., Nagahama, H., Yodogawa, E., 2006. Symmetropy of earthquake patterns: asymmetry and rotation in a disordered seismic source. Acta. Geophys. 54, 3-14.

Nishiyama, Y., Nanjo, K.Z., Yamasaki, K., 2008. Geometrical minimum units of fracture patterns in two-dimensional space: lattice and discrete Walsh functions. Physica A 387, 6252-6262.

Rosen, J., and Copie, P., 1982. On symmetry in physical phenomena, symmetry of an electric field and of a magnetic field: an English translation of Curie (1894). In: Rosen, J. (Eds.), Symmetry in Physics. American Association of Physics Teachers, New York, pp. 17-25.

Rutherford, J.S., 2001. A combined structure and symmetry classification of the urea series channel inclusion compounds. Cryst. Eng. 4, 269-281.

Turing, A.M., 1952. The chemical basis of morphogenesis. Philos. Trans. Roy. Soc. London B237, 37-72.

Wolfram, S., 2002. A New Kind of Science. Wolfram Media, Champaign, IL.

Yamasaki, K., Nanjo, K.Z., 2009. A new mathematical tool for analyzing the fracturing process in rock: partial symmetropy of microfracturing. Phys. Earth Planet. In. 173, 297-305.

Yodogawa, E., 1982. Symmetropy, an entropy-like measure of visual symmetry. Percept. Psychophys. 32, 230-240.

Figure captions

Fig. 1. Conceptual diagrams of Fourier analysis (A) and discrete Walsh analysis (B). The coefficients are spectrum.

Fig. 2. Patterns obtained by computer simulation of cell sorting system (data from Mochizuki et al., 1996). A part (40×40) of whole simulation space (100×100) is shown. Each simulation is executed from a random initial pattern for 10000 time steps. Parameters are: $m = 0.5$, and relative differential adhesion is: (A) $A/m = -2$; (B) $A/m = -1$; (C) $A/m = 0$; (D) $A/m = 0.6$; (E) $A/m = 1.2$; (F) $A/m = 2$; (G) $A/m = 4$; (H) $A/m = 6$.

Fig. 3. Pattern formation in mussels under experimental laboratory conditions (data from Koppel et al., 2008).

Fig. 4. (A) Examples of the two-dimensional discrete Walsh function for $M = N = 4$. Black and white represent $+1$ and -1, respectively. (B) Four types of symmetry in the sense of the discrete Walsh function.

Fig. 5. Entropy (E_n) and symmetropy (S) of samples. The full meanings of the numbers (i), (ii) and (iii) are described in Section 4. (i) The pattern becomes systematic (E_n decreases) with the predominance of the particular symmetry (S also decreases). (ii) The pattern becomes random (E_n increases) to maintain the degree of symmetry (constant S). (iii) The pattern restores the particular symmetry (S decreases) to maintain the randomness (constant E_n).

Fig. 6. Normalized power spectrum of Fig. 2. (A)-(H) in this figure correspond to (A)-(H) in Fig. 2, respectively.

Fig. 7. Plots of entropy, symmetropy and four types of symmetry for cell sorting against A/m. The data at $A/m = -2$: $P_1 = 0.03$, $P_2 = 0.02$, $P_3 = 0.92$, $P_4 = 0.03$, $S = 0.54$ and $E_n = 0.15$ are not plotted in the figures, because they are quite different from the other data.

Fig. 8. Plots of entropy, symmetropy and four types of symmetry for pattern formation in mussels against time.

Fig1

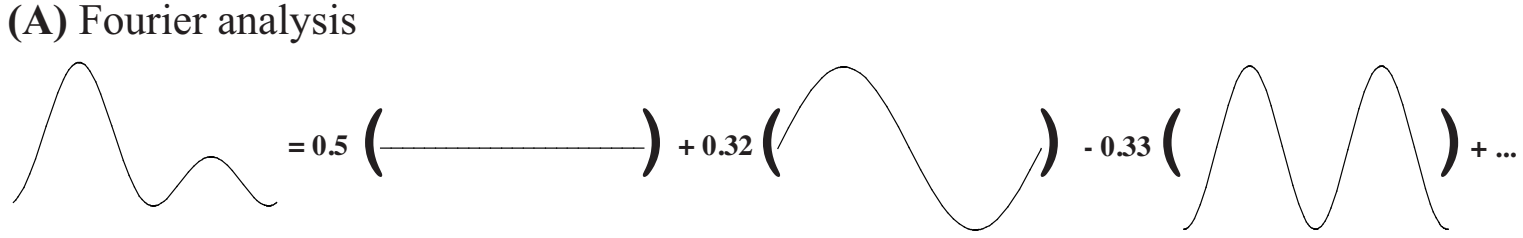
(A) Fourier analysis
= 0.5
+ 0.32
- 0.33
+ ...

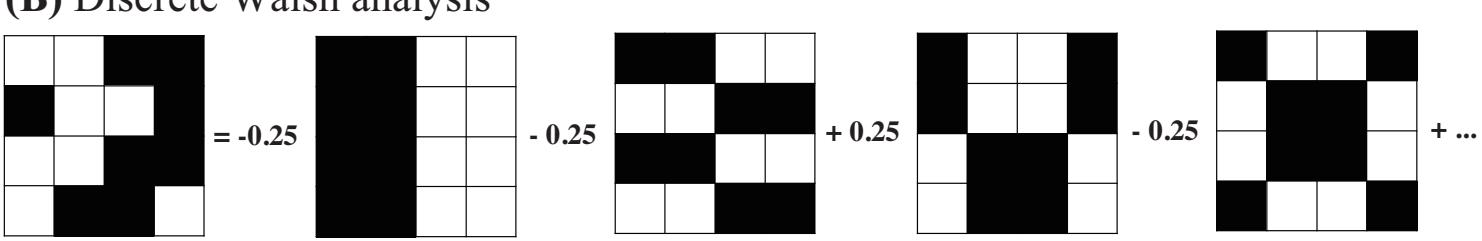
(B) Discrete Walsh analysis
= -0.25
- 0.25
+ 0.25
- 0.25
+ ...

Fig2

(A) $A/m = -2$

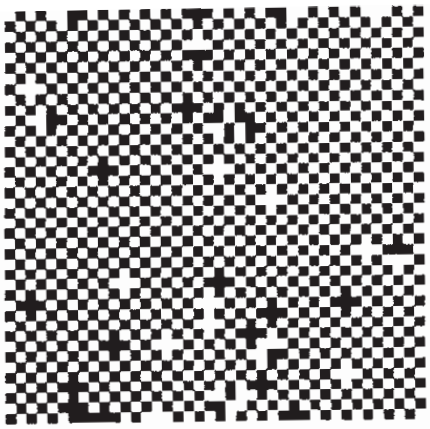

(B) $A/m = -1$

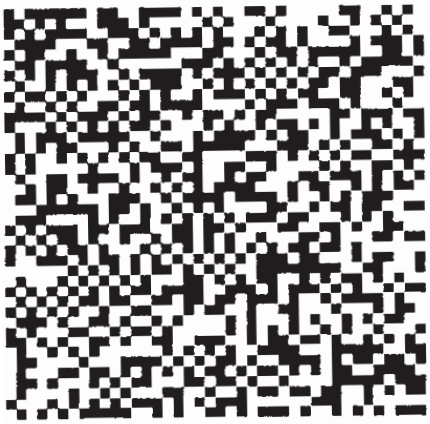

(C) $A/m = 0$

(D) $A/m = 0.6$

(E) $A/m = 1.2$

(F) $A/m = 2$

(G) $A/m = 4$

(H) $A/m = 6$

Fig3

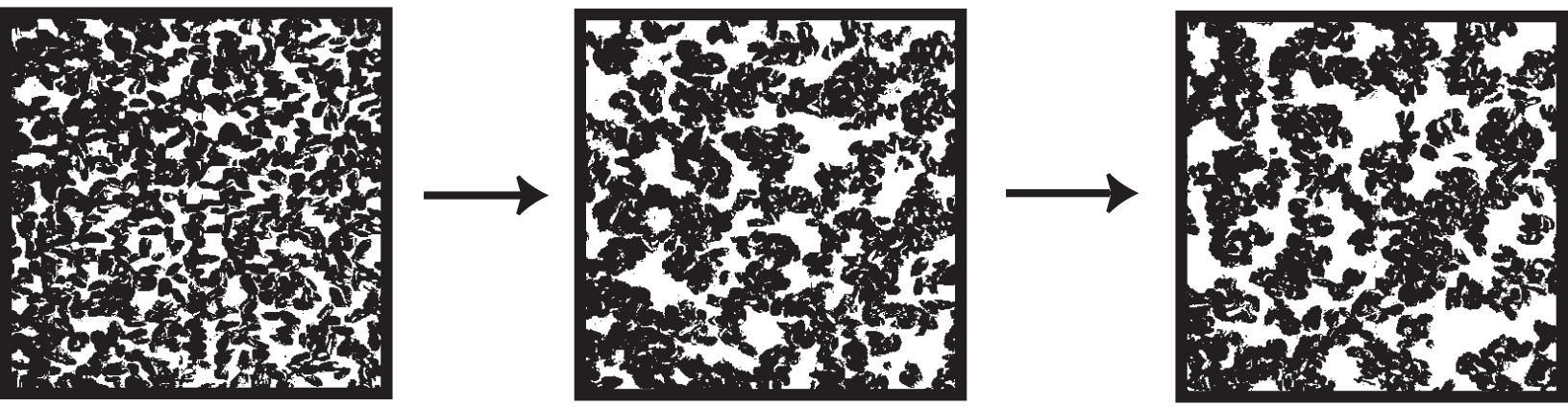

Fig4

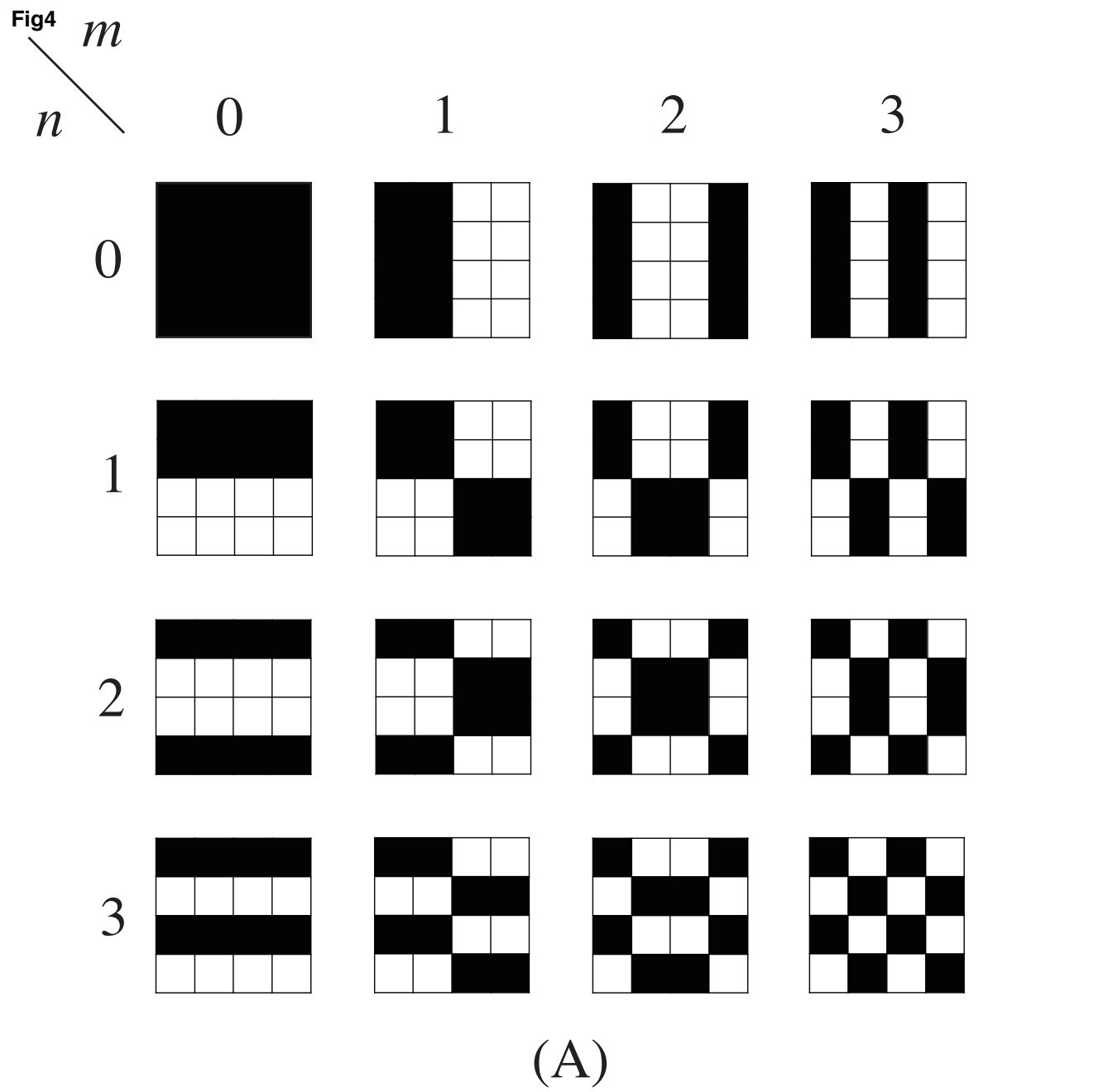
m
n
0
1
2
3
0
1
2
3

(A)

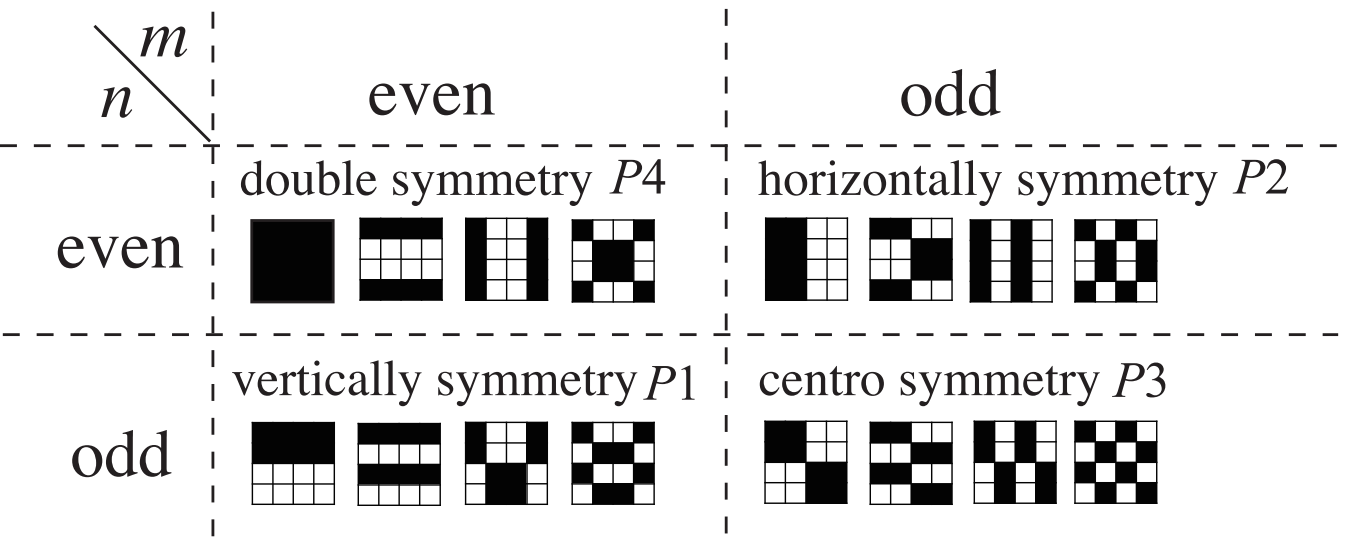
m
n
even
odd
double symmetry P4
horizontally symmetry P2
vertically symmetry P1
centro symmetry P3
even
odd

(B)

Fig5

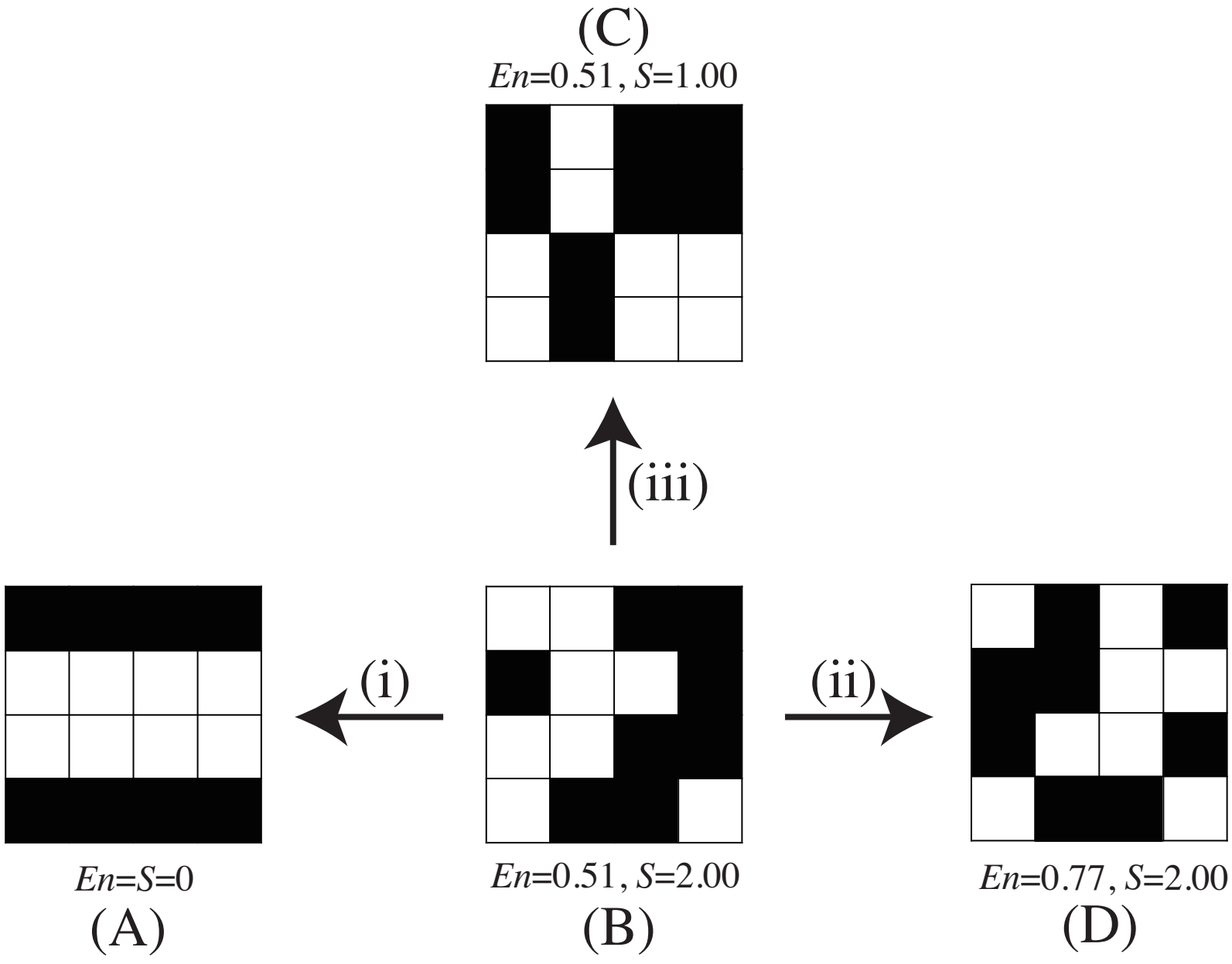

Fig6

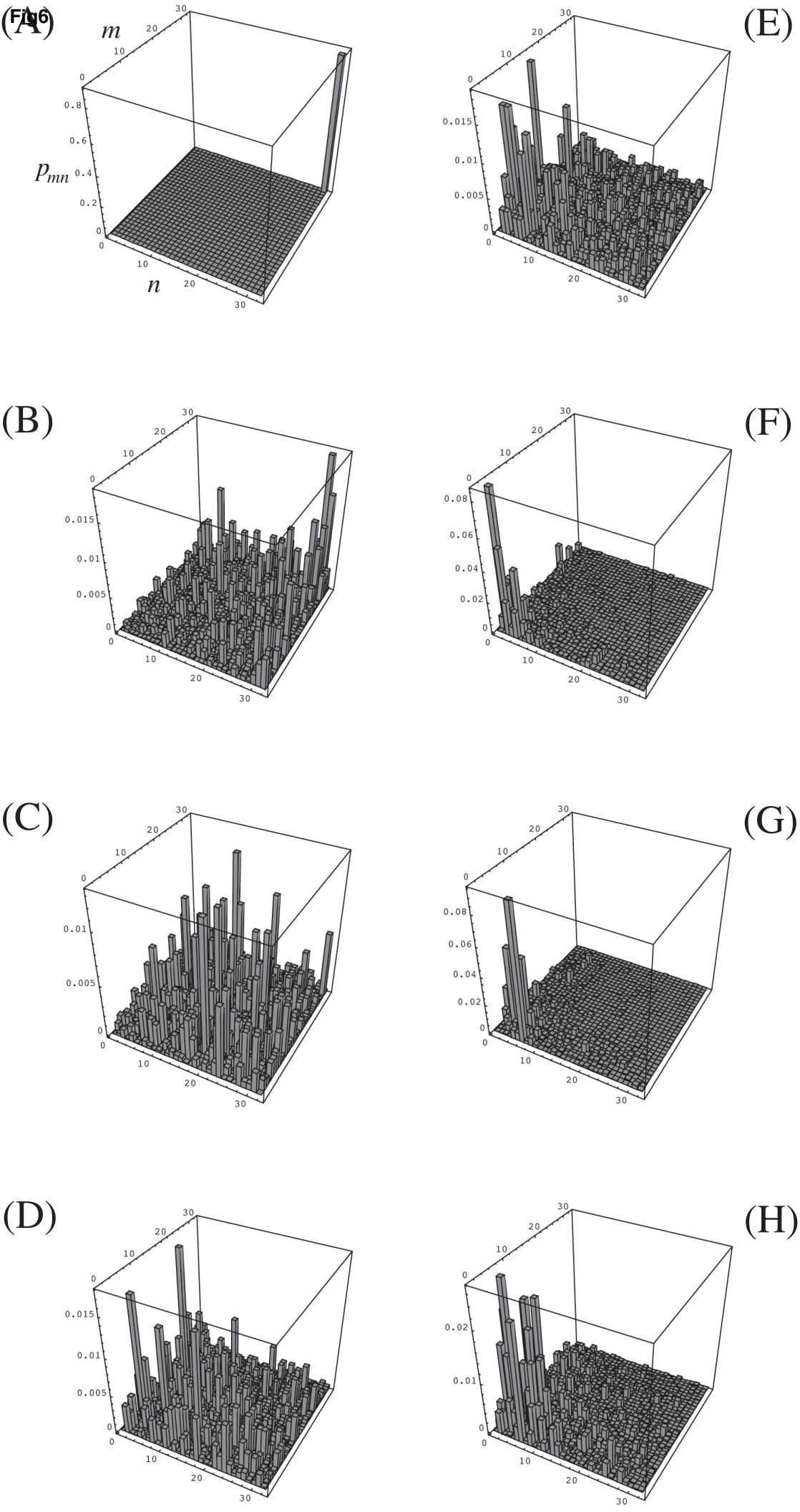

Fig7

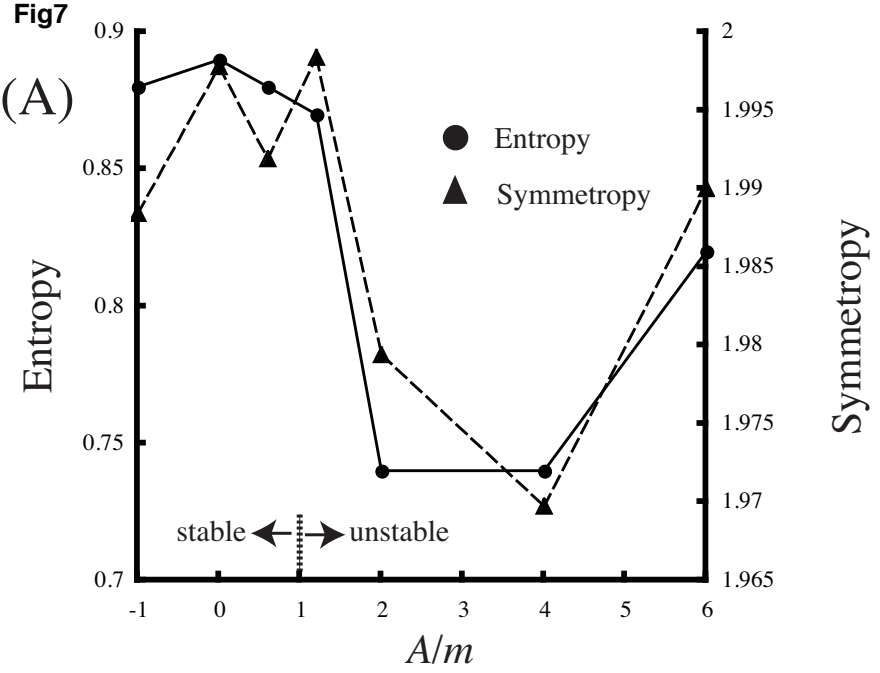
(A)
Entropy
Symmetropy
stable
unstable
A/m

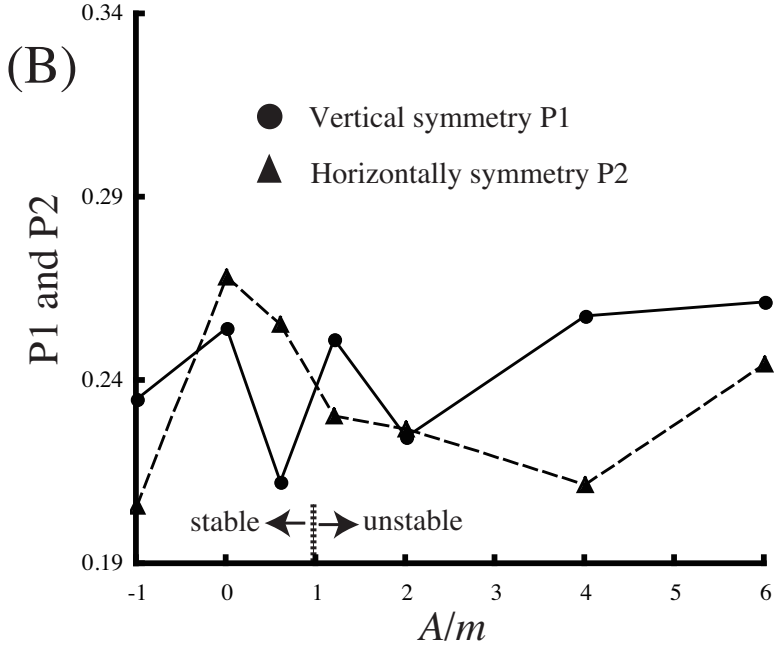
(B)
Vertical symmetry P1
Horizontally symmetry P2
P1 and P2
stable
unstable
A/m

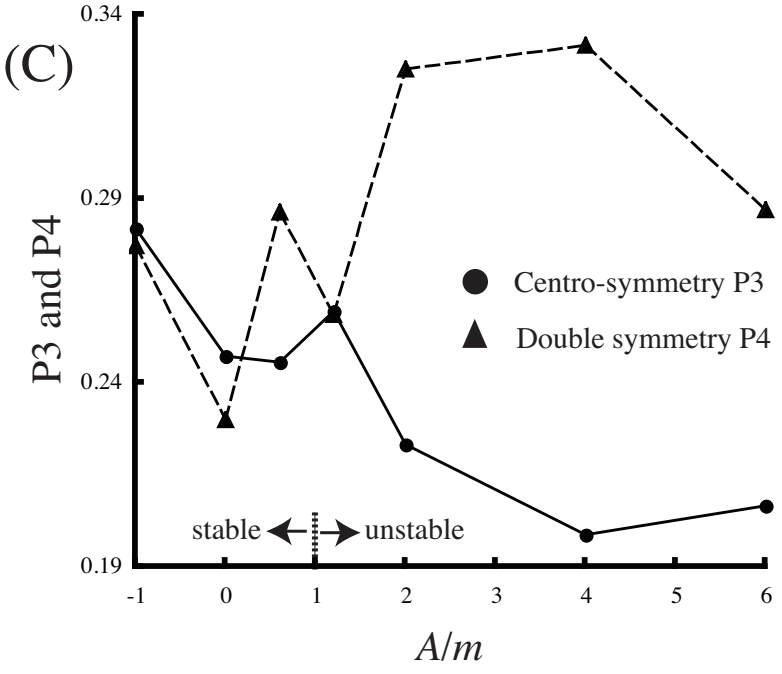
(C)
Centro-symmetry P3
Double symmetry P4
P3 and P4
stable
unstable
A/m

Fig8

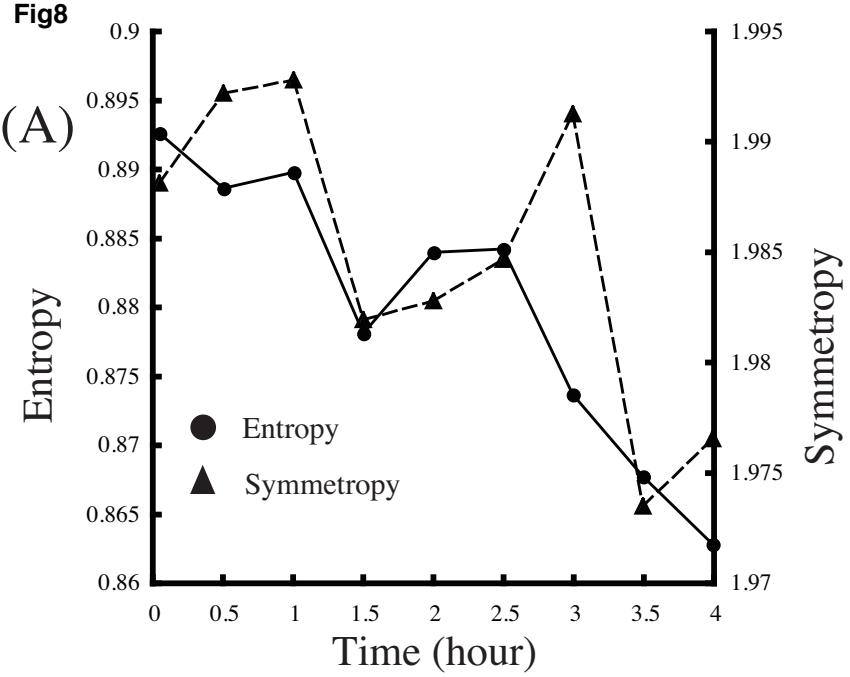
(A)
Entropy
Symmetropy
Entropy
Symmetropy
Time (hour)

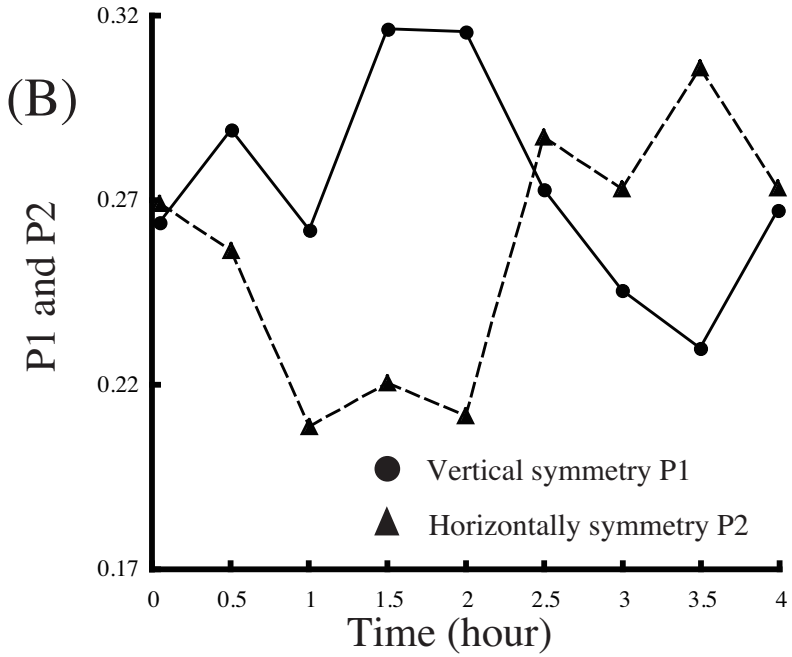
(B)
P1 and P2
Vertical symmetry P1
Horizontally symmetry P2
Time (hour)

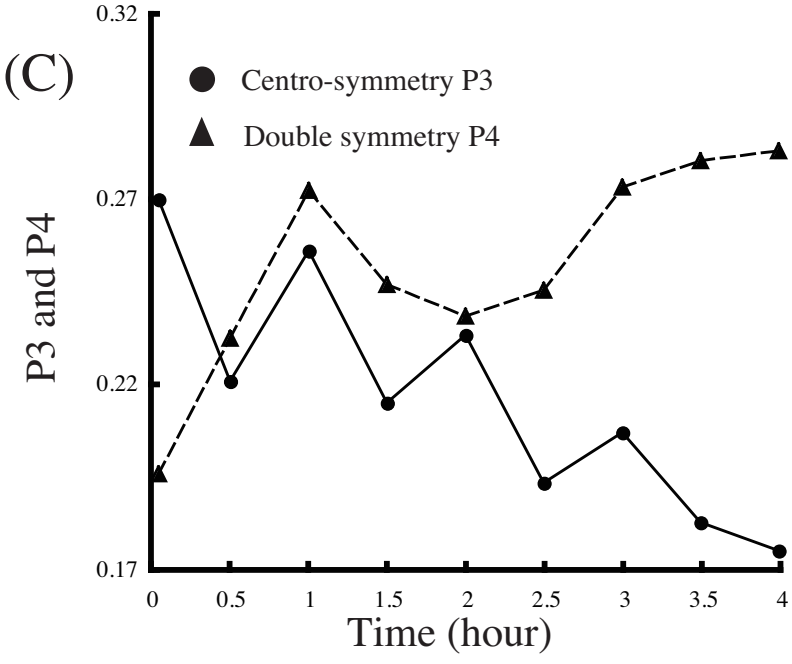
(C)
P3 and P4
Centro-symmetry P3
Double symmetry P4
Time (hour)